k-ε Turbulence Modeling in the CUPID Code for Natural Convection

Seung-Jun Lee[a*], Ik Kyu Park[a], Han Young Yoon[a], Jungwoo Kim[b]
[a]*Thermal Hydraulics Safety Department, Korea Atomic Energy Research Institute*
1045 Daedeok-daero, Yuseong-gu, Daejeon, 305-353, Republic of Korea
[b]*Mechanical System Design Engineering Department, Seoul National University of Science and Technology,*
232, Gongneung-ro, Nowon-gu, Seoul, 139-743, Republic of Korea
[*]*Corresponding author: cosinesj@kaeri.re.kr*

1. Introduction

The multi-dimensional two-fluid thermal hydraulics code, CUPID, has been developed in KAERI [1] and intensively used in analysing the two-phase phenomena in the nuclear reactor components [2-5]. Recently, passive cooling systems have been spotlighted because of its inherent safety feature. Thus, the natural convection phenomena in a pool have been studied using the CUPID code [6-7]. However, all the studies were focused on validating the computational ability on the simulation of the complicated two-phase phenomena in the liquid cooling tank qualitatively. To investigate the thermal mixing phenomena in pools quantitatively and to be utilized in designing those passive two-phase systems, a more sophisticated evaluation on the methodologies used in natural convection analysis should be validated.

In this study the turbulence model of CUPID is tested, which is the crucial factor influencing the thermal mixing in a pool. The standard k-e turbulence model and the low-Reynolds-number k-e turbulence model are tested against the thermally driven cavity experimental data [8]. By the local Nusselt number, temperature and velocity distribution, the performance of the models are compared.

2. The CUPID Code

A transient two-fluid, three-field model is adopted in the CUPID code where the three-field means vapor, continuous liquid and droplet fields. A major application of the CUPID code is the analysis of transient two-phase flow with a resolution ranging from the CFD scale to the component scale. To close the three field equations, several physical models are applied according to the simplified flow topology map.

2.1 Governing Equations

Separate conservation equations of mass, momentum and energy are established for the three fields. The mass and momentum equations for the *k*-field are:

$$\frac{\partial}{\partial t}\left(\alpha_k\rho_k\right)+\nabla\cdot\left(\alpha_k\rho_k\vec{u}_k\right)=\Omega_k\,, \tag{1}$$

$$\begin{aligned}&\frac{\partial}{\partial t}\left(\alpha_k\rho_k\vec{u}_k\right)+\nabla\cdot\left(\alpha_k\rho_k\vec{u}_k\vec{u}_k\right)=\\&-\alpha_k\nabla P+\nabla\cdot\left[\alpha_k\left(\mu_l+\mu_t\right)\nabla\vec{u}_k\right]+\alpha_k\rho_k\vec{g}\,.\\&+\mathbf{M}_k^{mass}+\mathbf{M}_k^{drag}+\mathbf{M}_k^{ndrag}+\mathbf{M}_k^{VM}\end{aligned} \tag{2}$$

The energy conservation equations for the gas and liquid field are:

$$\begin{aligned}&\frac{\partial}{\partial t}\left(\alpha_g\rho_g e_g\right)+\nabla\cdot\left(\alpha_g\rho_g e_g\vec{u}_g\right)=\\&-P\frac{\partial\alpha_g}{\partial t}-P\nabla\cdot\left(\alpha_g\vec{u}_g\right)+\ddot{q}_g+\nabla\cdot\left(\alpha_g\vec{q}_g\right)\end{aligned}\,, \tag{3}$$

$$\begin{aligned}&\frac{\partial}{\partial t}\left\{\left(\alpha_l+\alpha_d\right)\rho_l e_l\right\}+\nabla\cdot\left(\alpha_l\rho_l e_l\vec{u}_l+\alpha_d\rho_d e_d\vec{u}_d\right)\\&=-P\frac{\partial\left(\alpha_l+\alpha_d\right)}{\partial t}-P\nabla\cdot\left(\alpha_l\vec{u}_l+\alpha_d\vec{u}_d\right)\\&\quad+\ddot{q}_l+\nabla\cdot\left(\alpha_l\vec{q}_l+\alpha_d\vec{q}_d\right)-\Gamma_v h_f^*\\&\quad+H_{if}\left[T^s\left(P_s\right)-T_l\right]+\left(\frac{P-P_s}{P}\right)H_{gf}\left(T_g-T_l\right)\end{aligned}\,. \tag{4}$$

All the details of the parameters can be found in [9].

The density and temperature of each phase are expressed as functions of the independent variables, the pressure and internal energy.

$$\rho_l=\rho_l\left(P,e_l\right)\,, \tag{5}$$

$$T_l=T_l\left(P,e_l\right)\,. \tag{6}$$

The properties for the gaseous phase are calculated assuming a modified Gibbs-Dalton mixture of vapor and an ideal non-condensable gas:

$$\rho_v=\rho_v\left(P,e_v,X_n\right)\,, \tag{7}$$

$$T_v=T_v\left(P,e_v,X_n\right)\,, \tag{8}$$

$$\rho_s=\rho_s\left(P,e_v,X_n\right)\,. \tag{9}$$

The saturation temperature is represented as a function of the pressure:

$$T_{sat}=T_{sat}\left(P_s\right)\,. \tag{10}$$

2.2 Turbulence Model

For the turbulent shear stress in Eq. (2), liquid (or gas) shear-induced turbulence (μ_f^T, μ_g^T) model was used. The kinematic turbulence viscosities of gas and liquid are assumed to be equal [10].

$$\boldsymbol{\tau}_k^{\mathrm{Re}} = \mu_k^T \nabla \mathbf{v}_k \,, \tag{11}$$

$$\mu_f^T = C_\mu \rho_f k_f^2 / \varepsilon_f \,, \tag{12}$$

$$\mu_g^T = \mu_f^T \frac{\rho_g}{\rho_f} \,, \tag{13}$$

The turbulent flow is described using the Reynolds stress terms in Eq. (2) modeled with the $k-\varepsilon$ model. The two-fluid $k-\varepsilon$ transport equations are solved to obtain k_f , ε_f and k_g , ε_g where k_f and k_g mean the turbulent kinetic energy with the fluid and gas phase, and ε_f and ε_g mean the viscous dissipation rate. The two-fluid $k-\varepsilon$ transport equations are as follows:

$$\frac{\partial\left(\alpha_l \rho_l k_l\right)}{\partial t} + \nabla\cdot\left(\alpha_l \rho_l \vec{u}_l k_l\right) = \nabla\cdot\left[\alpha_l\left(\mu + \frac{\mu_t}{\sigma_k}\right)_l \nabla k_l\right] + \alpha_l P_{k,l} - \alpha_l \rho_l \varepsilon_l + \alpha_l P_{b,l} + \alpha_l S_k + \Phi + D \tag{14}$$

$$\frac{\partial\left(\alpha_g \rho_g k_g\right)}{\partial t} + \nabla\cdot\left(\alpha_g \rho_g \vec{u}_g k_g\right) = \nabla\cdot\left[\alpha_g\left(\mu + \frac{\mu_t}{\sigma_k}\right)_g \nabla k_g\right] + \alpha_g P_{k,g} - \alpha_g \rho_g \varepsilon_g + \alpha_g P_{b,g} + D \tag{15}$$

$$\frac{\partial\left(\alpha_l \rho_l \varepsilon_l\right)}{\partial t} + \nabla\cdot\left(\alpha_l \rho_l \varepsilon_l \vec{u}_l\right) = \nabla\cdot\left[\alpha_l\left(\mu + \frac{\mu_t}{\sigma_\varepsilon}\right)_l \nabla \varepsilon_l\right] + \frac{\alpha_l \varepsilon_l}{k_l}\left(f_1 C_{\varepsilon 1} P_{k,l} - f_2 C_{\varepsilon 2} \rho_l \varepsilon_l\right), \tag{16}$$
$$+ \frac{\varepsilon_l}{k_l} f_1 C_{\varepsilon 2} C_{\varepsilon 3} P_{b,l} + \alpha_l S_\varepsilon + E$$

$$\frac{\partial\left(\alpha_g \rho_g \varepsilon_g\right)}{\partial t} + \nabla\cdot\left(\alpha_g \rho_g \varepsilon_g \vec{u}_g\right) = \nabla\cdot\left[\alpha_g\left(\mu + \frac{\mu_t}{\sigma_\varepsilon}\right)_g \nabla \varepsilon_g\right] + \frac{\alpha_g \varepsilon_g}{k_g}\left(f_1 C_{\varepsilon 1} P_{k,g} - f_2 C_{\varepsilon 2} \rho_g \varepsilon_g\right), \tag{17}$$
$$+ \frac{\varepsilon_g}{k_g} f_1 C_{\varepsilon 2} C_{\varepsilon 3} P_{b,g} + E$$

where P_k , the shear production, is defined $\mu_t \sqrt{2 S_{ij} S_{ij}}$. S_{ij} is the modulus of the mean rate-of-strain tensor. S_k is the bubble motion kinetic energy source and Φ is the wall boiling kinetic energy source.

For natural convection, the buoyancy effect must be considered. Then $P_b = \beta \frac{\mu_T}{\mathrm{Pr}_T} \vec{g}\cdot\nabla T$ where β is the thermal expansion coefficient and is defined as

$$\beta = -\frac{1}{\rho}\left(\frac{\partial \rho}{\partial T}\right)_P \,. \tag{18}$$

Two versions of the $k-\varepsilon$ model are compared: standard $k-\varepsilon$ model with wall functions and Low-Reynolds-number $k-\varepsilon$ model of Chien [11].

Table I contains general coefficients for $k-\varepsilon$ models and Table II contains the additional coefficients for the low-Reynolds-number $k-\varepsilon$ model.

Table I: Coefficients for the two turbulence model

Coeffs.	standard	low-Reynolds-number
C_μ	0.09	1.44
$C_{\varepsilon 1}$	1.44	1.35
$C_{\varepsilon 2}$	1.92	1.80
σ_T	1.00	1.00
σ_k	1.00	1.00
σ_e	1.30	1.30

Table II: Additional Coefficients for the turbulence models

Coeffs.	standard	low-Reynolds-number
f_1	1	1.0
f_2	1	$1-\frac{2}{9}\exp\left(-(\mathrm{Re}_t/6)^2\right)$
f_μ	1	$1-\exp\left(-0.0115 y^+\right)$
D	0	$-2\mu k / y_n^2$
E	0	$-2\mu\frac{\varepsilon}{y_n^2}\exp\left(-0.5 y^+\right)$

For the coefficient, $C_{\varepsilon 3} = \tanh\left|\frac{V}{U}\right|$ [12] where V is the tangential velocity to the gravity and U is the normal direction to the gravity direction.

3. Simulation

Ampofo and Karayiannis' [8] experiment for natural convection is used for the validation of the turbulence models in the CUPID code. In their experiment, temperature, velocity and the local Nusselt number of air are obtained.

3.1 Problem Definition

Figure 1 shows the schematic figure of the experimental facility in two dimensions. Left and right walls are the heating surfaces and the others are adiabatic. The geometry is 0.75 m X 0.75 m. Hot and Cold wall temperatures are 323.15 *K* and 283.15 *K*, respectively. The turbulent Prandtl number is approximatedly 0.71. Rayleigh number is $1.58\text{x}10^9$. In their uncertainty estimation, air temperature is within 0.10 K, air velocity is 0.07 %, Nusselt number is 1.13% max.

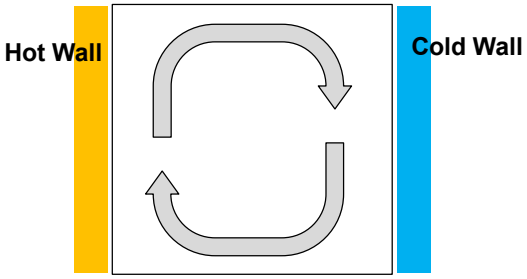

Fig. 1. A square cavity in natural convection.

The CUPID code uses the following two meshes. Figure 2a and 2b show the meshes for the standard model and the low-Reynolds-number model. The total cell number of both cases is 10,000. For the low-Reynolds-number model, the grid is clustered at walls to estimate the temperature and velocity gradient at wall well.

For the boundary condition, no pressure outlet is applied and the constant hot- and cold-wall conditions are used. For the initial conditions the flow properties are obtained from the mean temperature (303.15 *K*) condition.

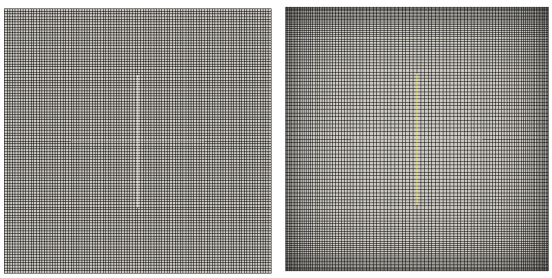

(a) Standard (b) low-Reynolds-number

Fig. 2. Grid generation for the standard and low-Reynolds-number model.

3.2 Simulation Results

According to [8], the thermal expansion coefficient can be arranged $\beta = Ra\alpha_m \nu_m / g\Delta TL^3$ from Rayleigh number definition so that $\beta \approx 0.003398$. Alternatively, depending on Bakakos' definition [13], $\beta = 1/T_m \approx 0.003299$. As shown in Fig. 3 the local thermal expansion coefficient (Eq. (18)) is in reasonable range when it is compared to the abovementioned values.

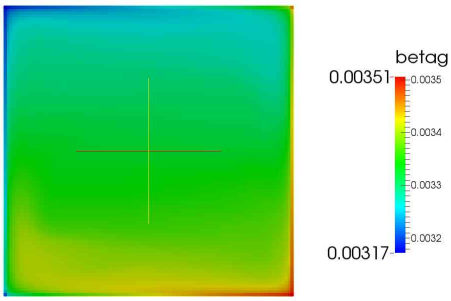

Fig. 3. Thermal expansion coefficient calculated from the steam table.

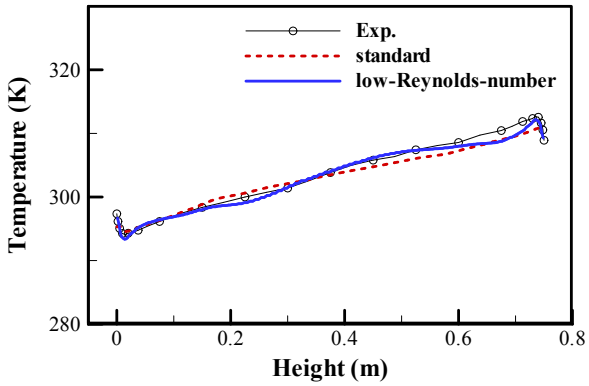

(a) Temperature at x=0.375 *m*

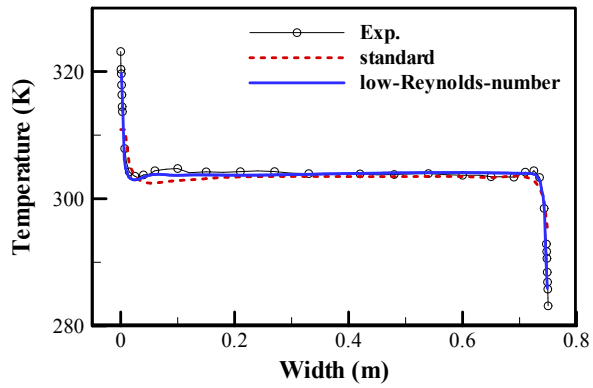

(b) Temperature at y=0.375 *m*

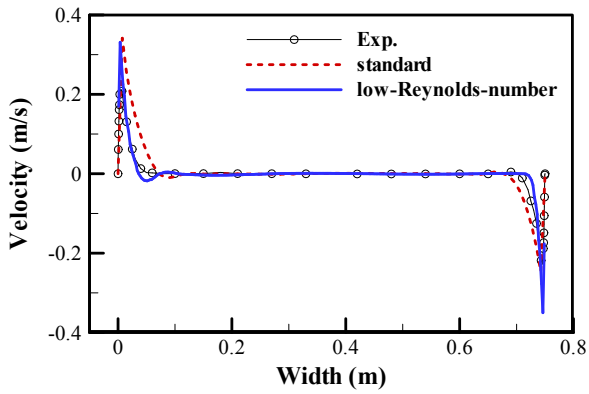

(c) Velocity at y=0.375 *m*

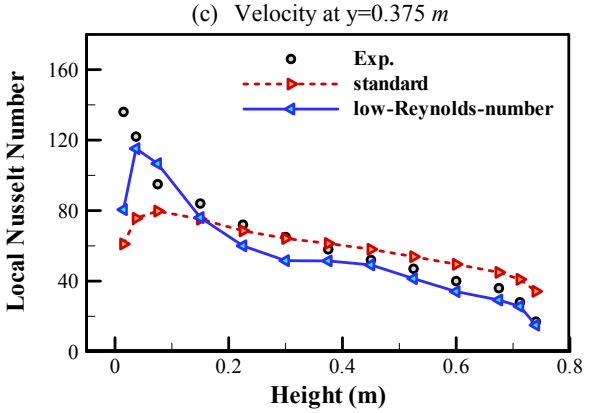

(d) Local Nusselt number at the hot wall

Fig. 4. Comparisons between the standard and low-Reynolds-number turbulence model.

Figure 4 shows the temperature, velocity and the local Nusselt number comparison between the standard and the low-Reynolds-number $k-\varepsilon$ model. Overall accuracy of the low-Reynolds-number model is better than the standard model. However, both models cannot predict the temperature and velocity profile at wall exactly. In Fig. 4d, the hot wall around the bottom show the maximum deviation. Since the Nusselt number is bigger when local fluid temperature is lower, the graph refers to a recirculation region in the corner. To resolve the recirculation flow, a finer grid would be recommendable. Moreover, Since Chien [11]'s low-Reynolds-number model is developed basically for simple nonseperating flows, such as channel flows, a model accounting for the corner effects in both attached and detached flows would show better results.

3. Conclusions

The standard and low-Reynolds-number $k-\varepsilon$ model are used to investigate natural convection phenomena in a square cavity using the CUPID code. The CUPID code is formulated from the basis of the steam table so that the local thermal expansion coefficient is used for the calculations. Throughout the simulations, the overall similarity was validated. However at walls the velocity is overpredicted and the temperature is underpredicted. Furthermore, the recirculation region is not resolved accurately. To achieve higher accuracy, any proper turbulence model can be recommended for CFD scale issues. However, for usual component scale problems, the thermal mixing estimation is globally acceptable.

ACKNOWLEDGMENT

This work was supported by the National Research Foundation of Korea (NRF) and the Korea Radiation Safety Foundation (KORSAFe) grant funded by the Korean government (MSIP & NSSC) (Nuclear Research and Development Program: 2012M2A8A4025647, Nuclear Safety Research Center Program: 1305011).

REFERENCES

[1] J.J. Jeong, K.S. Ha, B.D. Chung, and W.J. Lee, "Development of a multi-dimensional thermal-hydraulic system code, MARS 1.3.1," *Annals of Nuclear Energy*, vol. 26, no. 18, pp. 1611-1642, 1999.

[2] H.Y. Yoon, H.K. Cho, J.R. Lee, I.K. Park and J.J. Jeong, "Multi-scale thermal hydraulic analysis of PWRs using the CUPID code," *Nuclear Engineering and Technology*, Vol. 44, No.8, pp.831-846, 2012.

[3] H.Y. Yoon, J.R. Lee, H. Kim, I.K. Park, C.-H. Song, H.K. Cho, J.J Jeong, "Recent Improvements in the CUPID Code for a Multi-Dimensional Two-Phase Flow Analysis of Nuclear Reactor Components," *Nuclear Engineering and Technology,* Vol. 46, No.5, pp.655-666, 2014.

[4] H.Y. Yoon, J.J. Jeong, H.K. Cho, Y.S. Bang, K.W. Seul, "A Multi-scale analysis of the transient behavior of an advanced safety injection Tank," *Annals of Nuclear Energy*, vol. 62, pp. 17-25, 2013.

[5] J.J. Jeong, H.Y. Yoon, I.K. Park, and H.K. Cho, "The CUPID Code Development and Assessment Strategy," *Nuclear Engineering and Technology*, vol. 42, no. 6, pp. 636-655, 2010.

[6] H.K. Cho, S.J. Lee, H.Y. Yoon, K.-H. Kang, and J.J. Jeong, "Simulation of single- and two-phase natural circulation in the passive condensate cooling tank using the CUPID code," *Journal of Nuclear Science and Technology*, vol. 50, no. 7, pp. 709-722, 2013.

[7] S.J. Lee, H.K. Cho, K.H. Kang, S.Kim and H.Y, Yoon, "Numerical Analysis of the Passive Condensate Cooling Tank (PCCT) Using the CUPID Code," Proc. CFD4NRS-4 Daejeon, Korea, 2010.9.10-12.

[8] F. Ampofo and T.G. Karayiannis, "Experimental benchmark data for turbulent natural convection in an air filled square cavity," *International Journal of Heat and Mass Transfer*, Vol.46, pp.3551-3572, 2003.

[9] H. Kim, S.H. Kim, S.-J. Lee, I.K. Park, H.Y. Yoon, H.K. Cho, J.J. Jeong, "Development of CUPID-SG for the analysis of two-phase flows in PWR steam generators," *Progress in Nuclear Engineering*, Vol.77, pp.132-140, 2014.

[10] Y. Sato, K. Sekoguchi, "Liquid velocity distribution in two-phase bubble flow," *International Journal of Multiphase Flow,* **2**, 79-95, 1975.

[11] K.-Y. Chein, "Predictions of channel and boundary layer flows with a low-eynolds-number two-equation model of turbulence," AIAA-80-0134, 1980.

[12] W. Rodi, "Turbulence models and their application in hydraulics, a state of the art review," Int. Ass. For Hydraulic Research, Delft, The Netherlands, 1980.

[13] G. Barakos, E. Mitsoulis and D. Assimacopoulos, "Natural convection flow in a square cavity revisited: Laminar and turbulent models with wall functions," *International Journal for Numerical Methods in Fluids*, Vol. 18, pp.695-719, 1994.